

Arene Coordination in Bis(imino)pyridine Iron Complexes: Identification of Catalyst Deactivation Pathways in Iron-Catalyzed Hydrogenation and Hydrosilylation

Andrew M. Archer, Marco W. Bouwkamp, Maria-Patricia Cortez, Emil Lobkovsky, and Paul J. Chirik*

Department of Chemistry and Chemical Biology, Baker Laboratory, Cornell University, Ithaca, New York 14853

Received May 19, 2006

The phenyl-substituted bis(imino)pyridine iron bis(dinitrogen) complex (${}^i\text{PrPhPDI})\text{Fe}(\text{N}_2)_2$ (${}^i\text{PrPhPDI} = 2,6\text{-}(2,6\text{-}^i\text{Pr}_2\text{-C}_6\text{H}_3\text{N}=\text{CPh})_2\text{C}_5\text{H}_3\text{N}$) was prepared by sodium amalgam reduction of the corresponding ferrous dichloride precursor under 4 atm of dinitrogen. Comparison of the infrared stretching frequencies of the bis(dinitrogen), mono(dinitrogen), and related dicarbonyl derivatives to those of the corresponding bis(imino)pyridine iron compounds bearing the methyl-substituted ligand, (${}^i\text{PrPDI})\text{Fe}(\text{L})_n$ (${}^i\text{PrPDI} = 2,6\text{-}(2,6\text{-}^i\text{Pr}_2\text{-C}_6\text{H}_3\text{N}=\text{CMe})_2\text{C}_5\text{H}_3\text{N}$; $\text{L} = \text{CO}$, $n = 2$; $\text{L} = \text{N}_2$, $n = 1, 2$), established a more electrophilic iron center for the phenyl-substituted cases. Comparing the productivity of (${}^i\text{PrPhPDI})\text{Fe}(\text{N}_2)_2$ to (${}^i\text{PrPDI})\text{Fe}(\text{N}_2)_2$ in the catalytic hydrogenation and hydrosilylation of 1-hexene demonstrated higher turnover frequencies for (${}^i\text{PrPhPDI})\text{Fe}(\text{N}_2)_2$. For more hindered substrates such as cyclohexene and (+)-(R)-limonene, the opposite trend was observed, where the methyl-substituted precursor, (${}^i\text{PrPDI})\text{Fe}(\text{N}_2)_2$, produced more rapid conversion. The difference in catalytic performance resulted from competitive, irreversible formation of η^6 -aryl and -phenyl compounds with the phenyl-substituted complex. Addition of coordinating solvents such as cyclohexene or THF resulted in exclusive formation of the η^6 -phenyl derivative. When alkoxide substituents are introduced in the bis(imino)pyridine ligand backbone, the formation of η^6 -aryl compounds was exclusive, as alkali metal reduction of (${}^i\text{PrROPDI})\text{FeBr}_2$ (${}^i\text{PrROPDI} = 2,6\text{-}(2,6\text{-}^i\text{Pr}_2\text{-C}_6\text{H}_3\text{N}=\text{C}(\text{OR}))_2\text{C}_5\text{H}_3\text{N}$, $\text{R} = \text{Me}, \text{Et}$) yielded only the catalytically inactive η^6 -aryl species.

Introduction

Catalytic bond-forming reactions using well-defined coordination and organometallic compounds of iron are receiving increased attention given the relatively low cost and reduced environmental impact of the first-row metals compared to more precious second- and third-row counterparts.¹ Inspired by the reports of photocatalytic hydrogenation, hydrosilylation, and isomerization of olefins with $\text{Fe}(\text{CO})_5$ by Wrighton and co-workers,² our laboratory has been exploring modular, trivial to prepare, terdentate ligand scaffolds designed to mimic the proposed $[\text{Fe}(\text{CO})_3]$ active species.³ Aryl-substituted bis(imino)pyridine iron compounds are an attractive starting point given the large number of variants available by straightforward synthesis and precedent for catalytic C–C bond formation in olefin polymerization reactions.⁴

One significant challenge in developing iron catalysts is controlling unwanted one-electron redox changes, a problem not typically encountered with the second- and third-row congeners.⁵ Aryl-substituted bis(imino)pyridines are also useful in this regard, as the “redox activity”—the ability to accept up

to three electrons from the metal center⁶—is well-established for this ligand class.⁷ Our laboratory has recently described the synthesis and structural characterization of a bis(imino)pyridine iron bis(dinitrogen) complex, (${}^i\text{PrPDI})\text{Fe}(\text{N}_2)_2$ (${}^i\text{PrPDI} = 2,6\text{-}(2,6\text{-}^i\text{Pr}_2\text{-C}_6\text{H}_3\text{N}=\text{CMe})_2\text{C}_5\text{H}_3\text{N}$), **1**-(N_2)₂.⁸ Notably, **1**-(N_2)₂ serves as an efficient precatalyst for both the hydrogenation and hydrosilylation of olefins and alkynes (eq 1).⁸ **1**-(N_2)₂ has also been found to catalyze the hydrogenation of aryl azides to the corresponding anilines with isolable, crystallographically char-

(4) (a) Ittel, S. D.; Johnson, L. K.; Brookhart, M. *Chem. Rev.* **2000**, *100*, 1169. (b) Small, B. L.; Brookhart, M.; Bennett, A. M. A. *J. Am. Chem. Soc.* **1998**, *120*, 4049. (c) Britovsek, G. J. P.; Gibson, V. C.; Kimberley, B. S.; Maddox, P. J.; McTavish, S. J.; Solan, G. A.; White, A. J. P.; Williams, D. J. *Chem. Commun.* **1998**, 849. (d) Britovsek, G. J. P.; Bruce, M.; Gibson, V. C.; Kimberley, B. S.; Maddox, P. J.; Mastroianni, S.; McTavish, S. J.; Redshaw, C.; Solan, G. A.; Strömberg, S.; White, A. J. P.; Williams, D. J. *J. Am. Chem. Soc.* **1999**, *121*, 8728. (e) Gibson, V. C.; Spitzmesser, S. K. *Chem. Rev.* **2003**, *103*, 283. (f) Bianchini, C.; Mantovani, G.; Meli, A.; Migliacci, D.; Zanobini, F.; Laschi, F.; Sommazzi, A. *Eur. J. Inorg. Chem.* **2003**, 1620. (g) Bouwkamp, M. W.; Lobkovsky, E.; Chirik, P. J. *J. Am. Chem. Soc.* **2005**, *127*, 9660.

(5) Ingleson, M. J.; Pink, M.; Caulton, K. G. *J. Am. Chem. Soc.* **2006**, *128*, 4248.

(6) Enright, D.; Gambarotta, S.; Yap, G. P. A.; Budzelaar, P. H. M. *Angew. Chem., Int. Ed.* **2002**, *41*, 3873.

(7) (a) de Bruin, B.; Bill, E.; Bothe, E.; Weyhermüller, T.; Wieghardt, K. *Inorg. Chem.* **2000**, *39*, 2936. (b) Budzelaar, P. H. M.; de Bruin, B.; Gal, A. W.; Wieghardt, K.; van Lenthe, J. H. *Inorg. Chem.* **2001**, *40*, 4649. (c) Sugiyama, I.; Korobkov, I.; Gambarotta, S.; Mueller, A.; Budzelaar, P. H. M. *Inorg. Chem.* **2004**, *43*, 5771. (d) Scott, J.; Gambarotta, S.; Korobkov, I.; Knijnenburg, Q.; de Bruin, B.; Budzelaar, P. H. M. *J. Am. Chem. Soc.* **2005**, *127*, 17204.

(8) Bart, S. C.; Lobkovsky, E.; Chirik, P. J. *J. Am. Chem. Soc.* **2004**, *126*, 13794.

* To whom correspondence should be addressed. E-mail: pc92@cornell.edu.

(1) Bolm, C.; Legros, J.; Le Pailh, J.; Zani, L. *Chem. Rev.* **2004**, *104*, 6217.

(2) (a) Schroeder, M. A.; Wrighton, M. S. *J. Am. Chem. Soc.* **1976**, *98*, 551. (b) Schroeder, M. A.; Wrighton, M. S. *J. Organomet. Chem.* **1977**, *128*, 345.

(3) Kismartoni, L. C.; Weitz, E.; Cedenio, D. L. *Organometallics* **2005**, *24*, 4714.

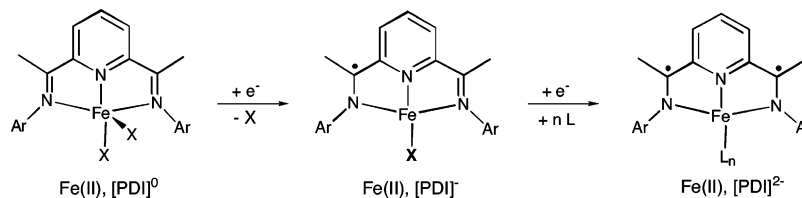


Figure 1. Redox-active bis(imino)pyridine ligands in iron chemistry.

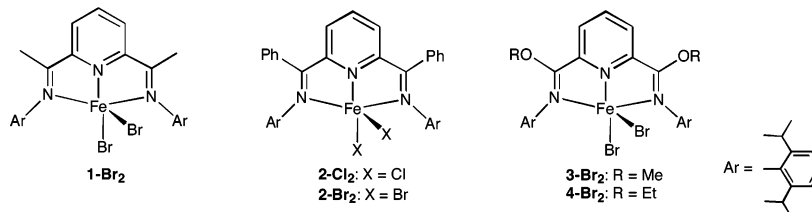
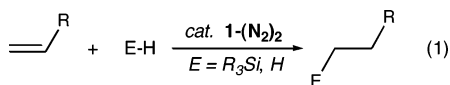


Figure 2. Bis(imino)pyridine iron dihalide precursors and the labeling scheme used in this study.

acterized bis(imino)pyridine iron imides serving as catalytically competent intermediates.⁹



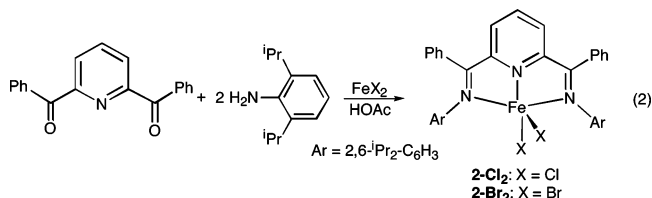
The electronic structures of $\mathbf{1-(N_2)_2}$ and related $\mathbf{1-(DMAP)}$ (DMAP = *N,N*-dimethylaminopyridine) have been more thoroughly investigated with Mössbauer spectroscopy and DFT calculations.¹⁰ These data, in combination with high-quality X-ray structures, establish intermediate spin ferrous ions ($S_{\text{Fe}} = 1$) complexed by a bis(imino)pyridine dianion, $[\text{PrPDI}]^{2-}$, where the singlet ($S_L = 0$) or triplet ($S_L = 1$) diradical are nearly isoenergetic (Figure 1). A doubly reduced bis(imino)pyridine chelate has also been observed by Gambarotta and co-workers with the synthesis and characterization of the square planar, paramagnetic iron methyl anion $[(\text{PrPDI})\text{FeMe}]^-$. While the magnetic data are not straightforward to interpret ($\mu_{\text{eff}} = 6.45 \mu_{\text{B}}$, 23 °C), both the metrical parameters and computational results support an intermediate spin Fe(II) center complexed to a two-electron-reduced bis(imino)pyridine dianion (Figure 1).¹¹

Having established the redox activity of the bis(imino)pyridine ligand in $\mathbf{1-(N_2)_2}$, we have become interested in exploring the role of ligand-centered radicals in catalysis. To address this issue and to further investigate the mechanism and scope of iron-catalyzed olefin hydrogenation and hydrosilation reactions, we have initiated a study whereby the electronic properties of the bis(imino)pyridine are systematically varied. By favoring (or disfavoring) the metal–ligand electron-transfer events, the catalytic activity may also be altered. In this contribution, we describe the introduction of phenyl and alkoxide substituents into the bis(imino)pyridine backbone and evaluation of the changes in structure, electronic properties, and catalyst performance. During the course of these investigations, an important catalyst deactivation pathway arising from intramolecular arene coordination has been identified.

Results and Discussion

Reduction of Phenyl-Substituted Bis(imino)pyridine Iron Dihalides. Phenyl- and alkoxide-substituted bis(imino)pyridines were chosen for this study, as straightforward synthetic routes to the desired compounds have been developed and the electronic properties are expected to differ from the original methyl-substituted compound.¹² In addition, replacement of the backbone methyl group with phenyl or alkoxide substituents

may protect the complex from unwanted deprotonation reactions.^{13,14} Each of the bis(imino)pyridine iron dihalide precursors used in this study are presented in Figure 2. The phenyl-substituted ferrous dihalides ($\text{PrPhPDI})\text{FeX}_2$ ($\text{PrPhPDI} = 2,6\text{-}(2,6\text{-}^i\text{Pr}_2\text{-C}_6\text{H}_3\text{N}=\text{CPh})_2\text{C}_5\text{H}_3\text{N}$; X = Cl, $\mathbf{2-Cl}_2$; X = Br, $\mathbf{2-Br}_2$) were prepared using a modification of a procedure originally reported by Esteruelas and co-workers¹⁵ involving a Schiff-base condensation of 2,6-diisopropylaniline with 2,5-dibenzoylpyridine in the presence of FeX_2 (eq 2). Both $\mathbf{2-Cl}_2$ and $\mathbf{2-Br}_2$ have also been synthesized by addition of the preformed bis(imino)pyridine with the appropriate iron(II) precursor.¹⁶



The alkoxide-substituted compounds ($\text{PrROPDI})\text{FeBr}_2$ ($\text{PrROPDI} = 2,6\text{-}(2,6\text{-}^i\text{Pr}_2\text{-C}_6\text{H}_3\text{N}=\text{C(OR)})_2\text{C}_5\text{H}_3\text{N}$, R = Me ($\mathbf{3-Br}_2$), Et ($\mathbf{4-Br}_2$)) were prepared as described previously.¹⁶ The 2,6-diisopropylaniline versions of the bis(imino)pyridines were used throughout this study for direct comparison to $\mathbf{1-(N_2)_2}$.

Reduction of either $\mathbf{2-Cl}_2$ or $\mathbf{2-Br}_2$ with an excess of 0.5% sodium amalgam under 4 atm of N_2 furnished the desired iron bis(dinitrogen) complex ($\text{PrPhPDI})\text{Fe(N}_2)_2$ ($\mathbf{2-(N_2)_2}$) (eq 3)). Four atmospheres of dinitrogen were necessary, as lower pressures led to unwanted side products arising from competitive arene coordination (vide infra).

(9) Bart, S. C.; Lobkovsky, E.; Chirik, P. J. *J. Am. Chem. Soc.* **2006**, *128*, 5302.

(10) Bart, S. C.; Chlopek, K.; Bill, E.; Bouwkamp, M. W.; Lobkovsky, E.; Neese, F.; Weighardt, K.; Chirik, P. J. Submitted.

(11) Scott, J.; Gambarotta, S.; Korobkov, I.; Budzelaar, P. H. M. *Organometallics* **2005**, *24*, 6298.

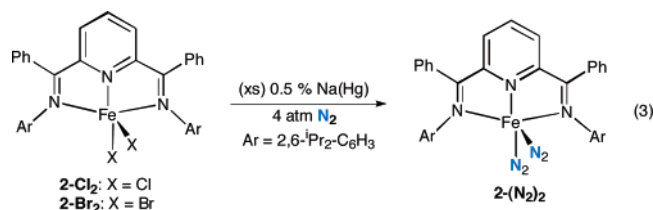
(12) Hansch, C.; Leo, A.; Taft, R. W. *Chem. Rev.* **1991**, *91*, 165.

(13) Bouwkamp, M.; Lobkovsky, E.; Chirik, P. J. *Inorg. Chem.* **2006**, *45*, 2.

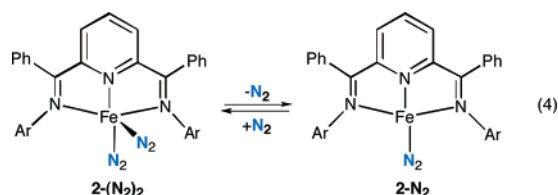
(14) Reardon, D.; Aharonian, G.; Gambarotta, S.; Yap, G. P. A. *Organometallics* **2002**, *21*, 786. (b) Sugiyama, H.; Aharonian, G.; Gambarotta, S.; Yap, G. P. A.; Budzelaar, P. H. M. *J. Am. Chem. Soc.* **2002**, *124*, 12268.

(15) Esteruelas, M. A.; López, A. M.; Méndez, L.; Oliván, M.; Oñate, E. *Organometallics* **2003**, *22*, 395.

(16) Kleigewe, N.; Steffen, W.; Blömker, T.; Kehr, G.; Fröhlich, R.; Wibbeling, B.; Erker, G.; Wasilke, J.-C.; Wu, G.; Bazan, G. *J. Am. Chem. Soc.* **2005**, *127*, 13955.



In analogy with $1\text{-(N}_2)_2$, dinitrogen coordination in $2\text{-(N}_2)_2$ is reversible. Stirring a pentane solution of $2\text{-(N}_2)_2$ for 20 min at 23 °C and collecting the noncombustible liberated gas with a Toepler pump produced a quantitative amount of dinitrogen (1 equiv) (eq 4). A second equivalent of N_2 gas was collected when the solution was stirred for an additional 48 h, arising from formation of a new bis(imino)pyridine iron product (vide infra). The interconversion of $2\text{-(N}_2)_2$ and 2-N_2 was also monitored by in situ infrared spectroscopy. In pentane solution at -78 °C, $2\text{-(N}_2)_2$ exhibited two intense $\text{N}\equiv\text{N}$ bands centered at 2086 and 2138 cm^{-1} . Upon warming, these bands gradually disappeared with concomitant growth of a new, single peak centered at 2061 cm^{-1} attributed to 2-N_2 . This process was reversible, as recooling the solution regenerated the bands for $2\text{-(N}_2)_2$.



The five-coordinate bis(imino)pyridine iron bis(dinitrogen) complex was also characterized by X-ray diffraction, combustion analysis, and NMR spectroscopy. A representation of the solid-state structure is presented in Figure 3 and establishes a pseudo-square pyramidal geometry with apical and basal N_2 ligands. Both dinitrogen ligands are weakly activated, with $\text{N}\equiv\text{N}$ bond lengths of 1.106(6) and 1.107(5) Å (Table 1), consistent with the solution IR stretching frequencies. As with $1\text{-(N}_2)_2$, the apical dinitrogen ligand is slightly bent, with an $\text{Fe}(1)\text{--N}(3)\text{--N}(4)$ bond angle of 170.4(5)°. A comparison of the solid-state structures of $1\text{-(N}_2)_2$ and $2\text{-(N}_2)_2$ (Figure 3) reveals little difference.

The bond distances in the bis(imino)pyridine ligand are consistent with two-electron reduction of the chelate.¹⁰ For example, the $\text{C}_{\text{imine}}\text{--N}_{\text{imine}}$ bond lengths are elongated to 1.355(7) and 1.344(7) Å while the $\text{C}_{\text{imine}}\text{--C}_{\text{ipso}}$ distances are

Table 1. Comparison of Selected Bond Distances (Å) and Angles (deg) for $1\text{-(N}_2)_2$ and $2\text{-(N}_2)_2$

	$1\text{-(N}_2)_2$	$2\text{-(N}_2)_2$
Fe(1)–N(1)	1.8341(16)	1.841(5)
Fe(1)–N(3)	1.8800(19)	1.865(5)
Fe(1)–N(5)	1.9452(16)	1.935(5)
Fe(1)–N(6)	1.8362(14)	1.842(4)
Fe(1)–N(7)	1.9473(16)	1.927(4)
N(1)–N(2)	1.090(2)	1.106(6)
N(3)–N(4)	1.104(3)	1.107(5)
C(2)–N(5)	1.332(2)	1.355(7)
N(6)–C(3)	1.376(2)	1.379(6)
N(6)–C(7)	1.367(2)	1.376(7)
C(8)–N(7)	1.333(2)	1.344(7)
C(2)–C(3)	1.428(3)	1.430(7)
C(7)–C(8)	1.427(2)	1.429(8)
Fe(1)–N(1)–N(2)	178.40(19)	178.5(5)
Fe(1)–N(3)–N(4)	171.81(17)	170.4(5)
N(1)–Fe(1)–N(3)	98.02(8)	99.0(2)
N(1)–Fe(1)–N(5)	96.65(7)	97.2(2)
N(1)–Fe(1)–N(7)	97.41(7)	96.6(2)
N(5)–Fe(1)–N(6)	74.49(6)	80.9(2)
N(6)–Fe(1)–N(7)	79.90(6)	79.3(2)

contracted to 1.430(7) and 1.429(8) Å as compared to the values in the corresponding iron dichloride compound where the ligand is in its neutral form.¹⁶ These values are consistent with population of molecular orbitals that are antibonding with respect to the imine but bonding with respect to the C–C backbone.¹⁰ Comparing these values to those for $1\text{-(N}_2)_2$ demonstrates similar distortions. Thus the structural data, coupled with the observed temperature independent paramagnetism (vide infra), suggest an intermediate spin ferrous ion with a bis(imino)pyridine dianion.

A relatively sharp and readily assignable ^1H NMR spectrum was observed over a 12 ppm chemical shift range for the equilibrium mixture of $2\text{-(N}_2)_2$ and 2-N_2 . As with 1-N_2 ,⁸ the resonances for the substituents orthogonal to the iron chelate plane are close to their diamagnetic reference values, while the hydrogens in the plane and hence in conjugation with the metal are more dramatically shifted. For example, the orthogonal, diastereotopic isopropyl methyl groups were observed at -0.71 and 1.16 ppm (1.04 and 1.27 in the free ligand), while the *p*-pyridine hydrogen appeared at -0.80 ppm (8.01 ppm in the free ligand).

Comparison of the Electronic Properties of Methyl- versus Phenyl-Substituted Bis(imino)Pyridine Iron Complexes. To compare the relative electronic environments imparted by the methyl- versus phenyl-substituted bis(imino)pyridine iron fragments, the synthesis of (*i*PrPhPDI)Fe(CO)₂ (2-(CO)_2) was

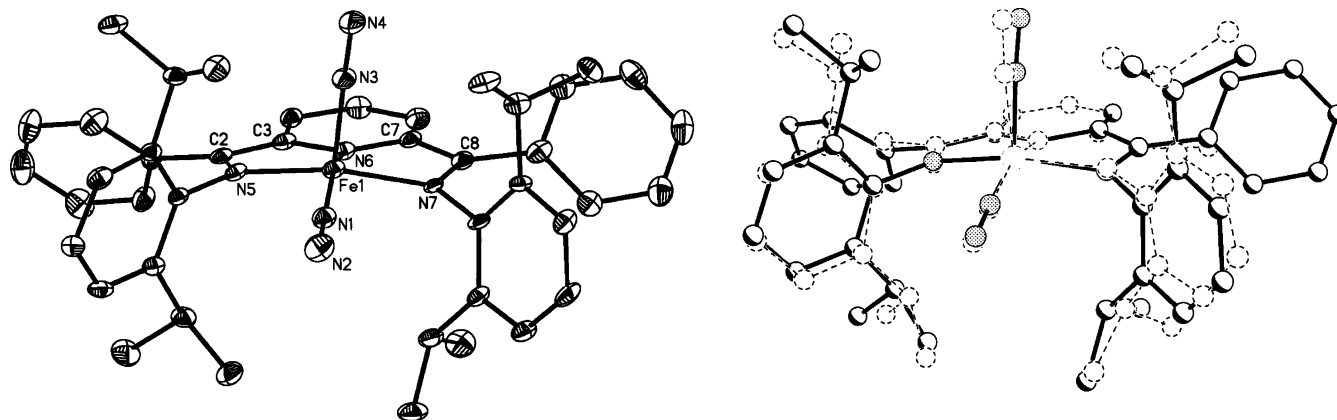


Figure 3. Molecular structure of $2\text{-(N}_2)_2$ with 30% probability ellipsoids (left). Overlay of the solid-state structures of $1\text{-(N}_2)_2$ (dashed) and $2\text{-(N}_2)_2$ (solid, right). Hydrogen atoms are omitted for clarity.

Table 2. Comparison of IR Spectroscopic Data for 1-(L)_n and 2-(L)_n Compounds

	1-(L) _n (cm ⁻¹)	2-(L) _n (cm ⁻¹)
$\nu(\text{N}_2)$ (pentane)	2073, 2132	2086, 2138
$\nu(\text{N}_2)$ (KBr)	2053, 2124	2074, 2130
$\nu(\text{N}_2)$ (pentane) ^a	2046	2061
$\nu(\text{CO})$ (pentane)	1914, 1974	1921, 1979

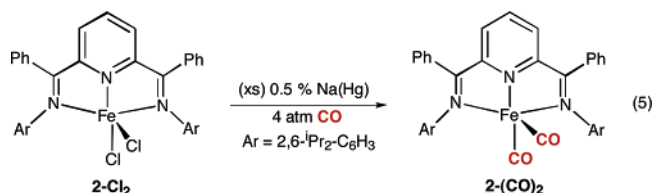
^a Value for the four-coordinate bis(imino)pyridine iron mono(dinitrogen) complex.

Table 3. Performance of 2-(N₂)₂ in Catalytic Olefin Hydrogenation and Hydrosilation and Comparison to 1-(N₂)₂

compound	hydrogenation TOF (h ⁻¹) ^a		hydrosilation TOF (h ⁻¹)	
	2-(N ₂) ₂	1-(N ₂) ₂	2-(N ₂) ₂	1-(N ₂) ₂
1-hexene	5300	3300	930	330
cyclohexene	60	1075	16	20
(R)-(+)-limonene	275	1085	37	166

^a Conditions: 0.3 mol % Fe, 1.25 M substrate in pentane solution at 22 °C. Hydrogenation reactions were conducted at 4 atm H₂, hydrosilations with 2 equiv of PhSiH₃.

undertaken. Exposure of 2-(N₂)₂ to 4 atm of carbon monoxide followed by solvent removal furnished a brown solid identified as 2-(CO)₂ on the basis of NMR and IR spectroscopies and combustion analysis. This compound was more routinely prepared by sodium amalgam reduction of 2-Cl₂ in the presence of carbon monoxide (eq 5).



Compiled in Table 2 are the dinitrogen and carbonyl infrared stretching frequencies for 1-(L)_n and 2-(L)_n. Comparing the pentane solution carbonyl bands reveals a 5 and 7 cm⁻¹ shift to higher frequencies upon substitution of a phenyl group for the methyl substituent. A similar trend is observed with the N₂ stretches, as 1-(N₂)₂ has lower frequency bands centered at 2073 and 2132 cm⁻¹ compared to the values of 2086 and 2138 cm⁻¹ for 2-(N₂)₂. In general, the bands for complexes with the phenyl-substituted backbone appear at *higher* frequency than those with the methyl backbone, suggesting more electrophilic iron centers in compounds bearing the [PrPhPDI] ligand.

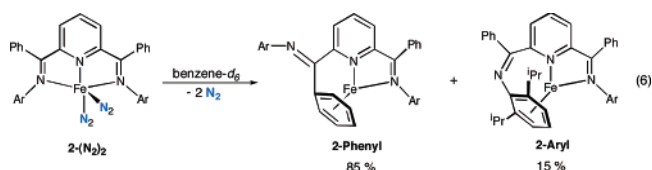
Catalytic Activity of 2-(N₂)₂ in Olefin Hydrogenation and Hydrosilation. The catalytic activity of the more electrophilic, phenyl-substituted complex, 2-(N₂)₂, was evaluated in a series of olefin hydrogenation and hydrosilation reactions. The hydrogenation reactions were conducted under standard conditions⁸ with 0.3 mol % iron at 22 °C in a 1.25 M pentane solution of the desired substrate. Typically 4 atm of H₂ were used; lower pressures were effective but not used for comparative purposes to avoid complications from mass-transfer effects. The catalytic hydrosilation reactions were also conducted with 0.3 mol % of 2-(N₂)₂ with a 1.25 M solution of substrate and 2 equiv of PhSiH₃.

As an initial catalytic assay, the hydrogenation and hydrosilation of three representative substrates, 1-hexene, cyclohexene, and (+)-(*R*)-limonene, were examined (Table 3). The progress of each catalytic reaction was monitored by gas chromatography, and the reported turnover frequencies are defined at >98% conversion (1-hexene) and after 60 min for cyclohexene and

(+)-(*R*)-limonene. For (+)-(*R*)-limonene, only the *geminal* olefin was reduced. As is typical for transition metal-catalyzed hydrosilation reactions,¹⁷ anti-Markovnikov addition of the silane to the olefin predominates. For 1-hexene, a 2:1 ratio of phenylsilane to olefin was required to obtain the monosilylated product. If lower concentrations of silane were employed, detectable quantities of the bis(alkylated) product, dihexyl-(phenyl)silane, were observed.

Comparing the relative productivities of 1-(N₂)₂ and 2-(N₂)₂ demonstrated that the phenyl-substituted compound was more productive for catalytic 1-hexene hydrogenation and hydrosilation but was inferior for the traditionally more difficult substrates such as cyclohexene and (+)-(*R*)-limonene. During the course of these investigations, it was discovered that the productivity of 1-(N₂)₂ was higher when pentane rather than toluene was used as the reaction medium. All of the turnover frequencies reported in Table 3 were determined in pentane solution.

Identification of Catalyst Deactivation Pathways: Characterization of η^6 -Aryl and η^6 -Phenyl Bis(imino)pyridine Iron Complexes. The difference in the relative hydrogenation and hydrosilation productivities of 1-(N₂)₂ and 2-(N₂)₂ suggested a competitive catalyst deactivation pathway for the phenyl-substituted complex. To investigate this possibility, the stability of 2-(N₂)₂ in benzene-*d*₆ was monitored as a function of time by ¹H NMR spectroscopy. Over the course of hours at 23 °C, clean and quantitative conversion to two new diamagnetic products in an 85:15 ratio was observed. A combination of multinuclear NMR spectroscopy, combustion analysis, and X-ray diffraction identified the new products as the bis(imino)pyridine iron η^6 -phenyl compound, 2-Phenyl (major, 85%), and the corresponding η^6 -2,6-diisopropylphenyl complex, 2-Aryl (minor, 15%, eq 6). Notably, both iron arene complexes were unreactive toward dihydrogen, silanes, and olefins. This behavior most likely accounts for the diminished catalytic productivity of 2-(N₂)₂ with more hindered substrates where longer times are required for complete conversion. The robust nature of the arene complexes was further demonstrated by the lack of a reaction with 4 atm of carbon monoxide upon heating to 80 °C over 24 h.



As we have reported previously with α -diimine iron compounds,¹⁸ η^6 -coordination of the arene ligand was readily identified by ¹H spectroscopy, as the peaks for the coordinated ring shift upfield relative to free arene. In benzene-*d*₆, the ¹H NMR spectrum of 2-Phenyl exhibited the number of peaks expected for a molecule with idealized C_s symmetry. Three upfield shifted phenyl resonances were identified at 3.85 (*para*), 5.32 (*meta*) and 5.66 (*ortho*) ppm. Similar spectroscopic features were observed for 2-Aryl, with two upfield shifted arene peaks centered at 4.36 ppm (*para*) and 5.63 ppm (*meta*). The ¹H and ¹³C NMR spectra for both compounds were completely assigned with the aid of two-dimensional NMR experiments and the peak listings are reported in the Experimental Section.

Both η^6 -aryl complexes were characterized by X-ray diffraction. The solid-state structures for 2-Phenyl and 2-Aryl are

(17) Jardine, F. H. *Prog. Inorg. Chem.* **1981**, 28, 63.

(18) Bart, S. C.; Hawrelak, E. J.; Lobkovsky, E.; Chirik, P. J. *Organometallics* **2005**, 24, 5518.

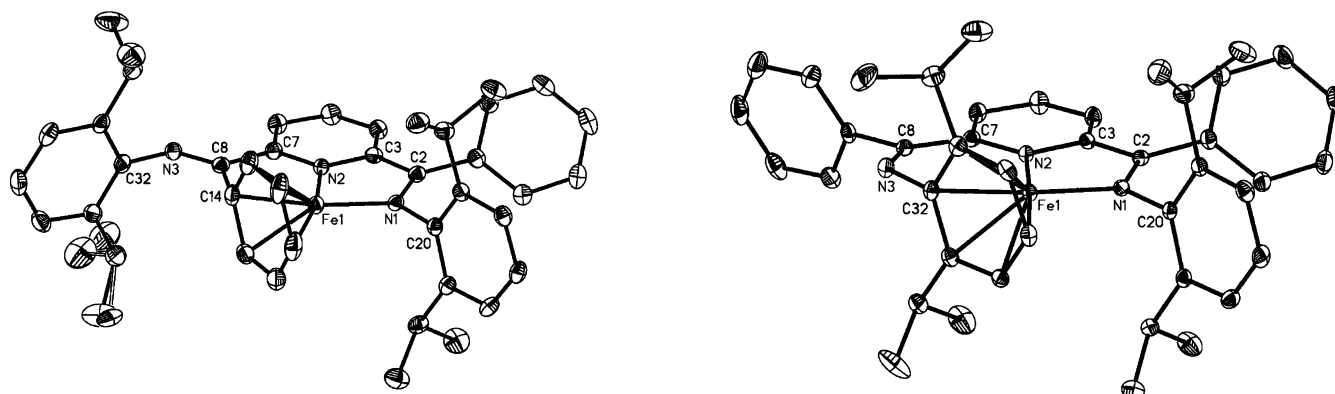


Figure 4. Molecular structure of **2-Phenyl** (left) and **2-Aryl** (right) with 30% probability ellipsoids. Hydrogen atoms are omitted for clarity.

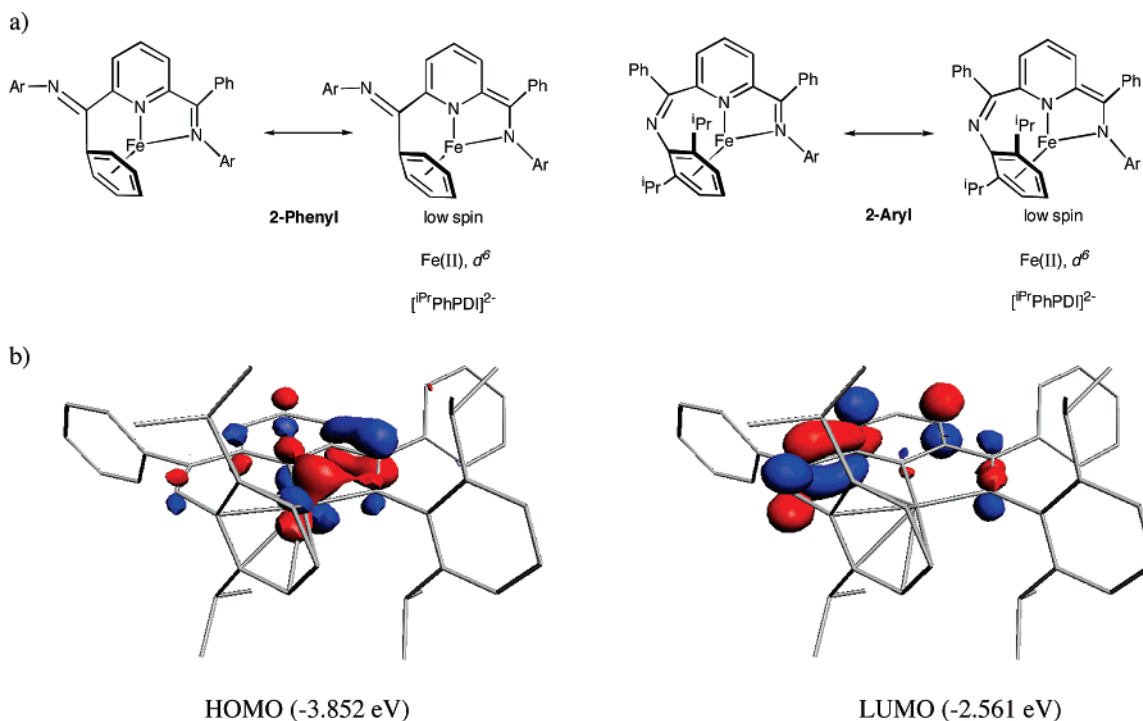


Figure 5. (a) Reduction of the bis(imino)pyridine ligands in **2-Aryl** and **2-Phenyl** and (b) DFT-computed HOMO (left) and LUMO (right) of **2-Aryl**.

presented in Figure 4. Selected metrical parameters are reported in Table 4. In the structure of **2-Phenyl**, one isopropyl group was positionally disordered and was successfully modeled. Significant localization of the pyridine ring and contracted C(2)–C(3) bond distances are observed in both compounds. These ligand distortions coupled with the observation of elongated N(1)–C(2) distances are indicative of two-electron reduction of the bis(imino)pyridine ligand.⁷ Because one arm of the chelate is dissociated in both compounds, the bond lengths associated with this portion of the ligand provide a useful internal reference for “unperturbed” imine bonds. Consistent with reduction, the N(1)–C(2) bond length in **2-Aryl** elongates to 1.351(3) Å, compared to 1.283(3) Å in the free imine and 1.297(4) Å in (iPrPDI)FeCl₂ (**1-Cl₂**).¹⁶ Similar features are observed in **2-Phenyl** with N(1)–C(2) bond elongation to 1.369(3) Å compared to 1.267(3) Å for the free imine. The C(2)–C(3) contractions of 1.419(3) and 1.414(3) Å for **2-Aryl** and **2-Phenyl** are similar to the distortions observed in the solid-state structures of α -diimine iron arene complexes.¹⁸ Thus, the metrical parameters in conjunction with the observed diamag-

netism establish the presence of a low-spin ferrous ion complexed by a two-electron-reduced bis(imino)pyridine ligand (Figure 5).

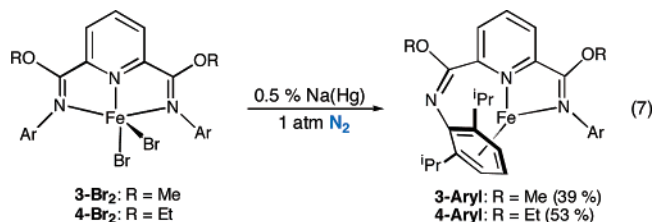
To confirm the formulation of the ligand as a bis(imino)pyridine dianion, the electronic structure of **2-Aryl** was further investigated with full molecule DFT calculations (ADF2003.01, TZ2P, ZORA). The optimized geometry is in excellent agreement with the experimentally determined solid-state structure. The frontier molecular orbitals are presented in Figure 5 and establish the involvement of the ligand. As has been noted previously,^{7,10} the LUMO of free aryl-substituted bis(imino)pyridine ligands are π -antibonding with respect to the C_{imine}–N_{imine} bond but π -bonding with respect to C_{ipso}–C_{imine}. Examination of the DFT-computed HOMO of **2-Aryl** demonstrates this feature and clearly establishes the doubly reduced, dianionic form of the chelate. Notably, the LUMO, which lies 29.8 kcal/mol above the HOMO, is a similar linear combination of ligand orbitals.

Reduction of Alkoxide-Substituted Bis(imino)pyridine Iron Dihalides. Attempts to prepare iron dinitrogen complexes bearing alkoxide-substituted bis(imino)pyridine ligands were

Table 4. Selected Metrical Parameters for 2-Aryl and 2-Phenyl

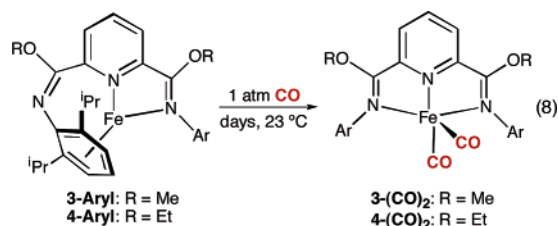
	2-Aryl	2-Phenyl
Fe(1)–N(1)	1.9033(16)	1.8956(18)
Fe(1)–N(2)	1.8798(16)	1.8478(18)
N(1)–C(2)	1.351(3)	1.369(3)
N(2)–C(3)	1.405(3)	1.369(3)
N(2)–C(7)	1.391(3)	1.380(3)
C(2)–C(3)	1.419(3)	1.414(3)
C(3)–C(4)	1.401(3)	1.414(3)
C(4)–C(5)	1.362(3)	1.364(4)
C(5)–C(6)	1.405(3)	1.405(3)
C(6)–C(7)	1.378(3)	1.361(3)
C(7)–C(8)	1.483(3)	1.485(3)
N(3)–C(8)	1.283(3)	1.267(3)
N(1)–Fe(1)–N(2)	83.02(7)	81.36(8)
C(2)–N(1)–Fe(1)	116.15(13)	116.29(15)
C(3)–C(2)–N(1)	112.62(17)	112.08(19)
C(7)–C(8)–N(3)	129.72(18)	120.1(2)
C(7)–C(8)–C(14)	112.95(17)	112.14(19)

unsuccessful. Reduction of either **3-Br₂** or **4-Br₂** with an excess of 0.5% sodium amalgam afforded red, diamagnetic products identified as the η^6 -arene compounds **3-Aryl** and **4-Aryl**, respectively, arising from displacement of the imine nitrogen by the *N*-aryl substituent (eq 7).



As with **2-Phenyl** and **2-Aryl**, both arene compounds were readily identified by multinuclear NMR spectroscopy. In benzene-*d*₆, the number of ¹H and ¹³C resonances expected for *C_s* symmetric molecules were observed where the mirror plane contains the iron center and results in distinct resonances for the inequivalent alkoxide, pyridine, and aryl environments. For **3-Aryl**, diagnostic upfield shifted aryl hydrogens were observed at 4.11 (*para*) and 5.53 (*meta*) ppm, while similar peaks, centered at 4.19 (*para*) and 5.57 (*meta*) ppm, were assigned for **4-Aryl**. The coordinatively saturated, diamagnetic arene compounds are robust molecules, failing to convert to the corresponding iron bis(dinitrogen) complexes upon exposure to N₂.

To evaluate the electronic environment imparted by the alkoxy-substituted bis(imino)pyridine ligands, the synthesis of the corresponding dicarbonyl compounds was targeted. Exposure of the iron aryl complexes **3-Aryl** and **4-Aryl** to 4 atm of carbon monoxide at ambient temperature resulted in slow displacement of the arene ligand to furnish the desired dicarbonyl derivatives **3-(CO)₂** and **4-(CO)₂** as green solids, respectively (eq 8).



Substitution of the arene in the alkoxy-substituted compounds **3-Aryl** and **4-Aryl**, but not in the phenyl-substituted compounds **2-Aryl** may be a result of the relative electronic density at the iron imparted by the different bis(imino)pyridine ligands.

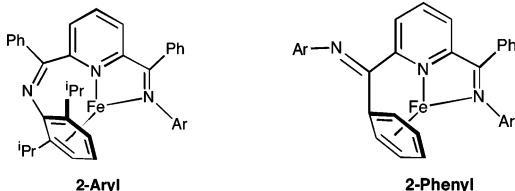
Because the metrical parameters and the DFT calculations on the η^6 -aryl compounds established little reduction and hence π -back-bonding to the arene, the iron–ring interaction is principally a σ -donation. As a result, the iron–arene bond is expected to be stronger in the more electron-deficient phenyl-substituted compound, **2-Aryl**, and hence would be less likely displaced by carbon monoxide.

Characterization of the bis(imino)pyridine iron dicarbonyl compounds by ¹H and ¹³C NMR spectroscopy established *C_{2v}* symmetric molecules, demonstrating that the carbonyl ligands are rapidly interchanging basal and apical positions by rocking through the iron chelate plane. Similar dynamic behavior was observed with related five-coordinate bis(imino)pyridine iron compounds.⁸ The pentane solution infrared spectrum of the ethoxy-substituted compound **4-(CO)₂** was straightforward to interpret, exhibiting two intense bands centered at 1972 and 1910 cm⁻¹. Comparing these values to those for **1-(CO)₂** and **2-(CO)₂** (Table 2) demonstrated that introduction of ethoxide substituents produced the most reducing bis(imino)pyridine iron complex to date.

The infrared spectrum of the methoxy-substituted complex exhibited *five* carbonyl bands, in contrast to the single *C_{2v}* symmetric product suggested by NMR spectroscopy. Two intense bands, centered at 1974 and 1912 cm⁻¹, are in agreement with those observed for **4-(CO)₂**. However, observation of another strong band at 2013 cm⁻¹ and two weaker bands at 1957 and 1933 cm⁻¹ suggest the presence of other isomers of the bis(imino)pyridine iron dicarbonyl compound. These additional peaks were observed in the same ratio from independently prepared samples that were >95% pure as judged by ¹H NMR spectroscopy.

While the experimental data are limited, we tentatively propose that the other bands arise from isomers where the oxygen atoms are coordinated to the iron rather than the imines. Thus, if both “ κ^3 -O,N,O” and “ κ^3 -O,N,N” isomers were also present, a total of *six* CO bands would be expected. Isomers involving a κ^2 -bis(imino)pyridine ligand also cannot be excluded. The observation of three additional bands suggests that two of the peaks overlap. The discrepancy between the NMR structure, which supports “ κ^3 -N,N,N” coordination, and the IR data, consistent with additional isomers in solution, may arise from the difference in time scales of the two experiments. As stated previously, **3-(CO)₂** is dynamic on the NMR time scale and may undergo dissociation of the imines in solution, resulting in observation of a time-average *C_{2v}* symmetric molecule. The IR time scale, being much shorter, may allow observation of the discrete components of the dynamic mixture. It should also be noted that oxygen coordination has been observed in the ferrous dihalide complex **3-Cl₂**.¹⁶ Observation of only two bands for **4-(CO)₂** suggests that introduction of a slightly larger ethyl group results in a more crowded oxygen atom that does not compete with the imine for the coordination sphere of the iron.

Insights into the Origin of η^6 -Arene Coordination. Because conversion of **2-(N₂)₂** to **2-Phenyl** and **2-Aryl** was identified as a major catalyst deactivation pathway, attempts were made to understand the origin of this deleterious reaction. Stirring a benzene or toluene solution of **2-(N₂)₂** under vacuum furnished predominantly **2-Phenyl** (85–90%) with small, yet detectable amounts (10–15%) of **2-Aryl**. Repeating the experiment in the presence of dinitrogen inhibited but did not prevent arene coordination. The half-life for the conversion of **2-(N₂)₂** into **2-Aryl** and **2-Phenyl** in benzene-*d*₆ under vacuum was approximately 7.5 h at 23 °C. Identical experiments performed

Table 5. Solvent Dependence for the Formation of 2-Aryl and 2-Phenyl at 23 °C


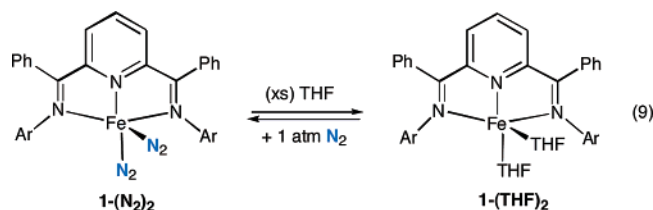
solvent ^a	% 2-Aryl	% 2-Phenyl
pentane	100	0
hexane	100	0
diethyl ether	100	0
mesitylene	100	0
benzene	15	85
toluene	10	90
THF	0	100
cyclohexene	0	100

^a All experiments stirred under vacuum for 48 h.

under 1 and 4 atm of dinitrogen produced half-lives of 19 and 125 h, respectively.

Changing the solvent medium to noncoordinating solvents such as pentane, hexane, diethyl ether, or mesitylene produced exclusively **2-Aryl** after 48 h at 23 °C (Table 5). In more coordinating solvents such as THF or cyclohexene, **2-Phenyl** was observed exclusively. Significantly, isolated and purified samples of **2-Phenyl** and **2-Aryl** did not interconvert in benzene-*d*₆ solution, even upon heating to 80 °C, demonstrating that arene coordination is irreversible. Similar observations were made in α -diimine iron arene chemistry where the perprotio α -diimine iron η^6 -benzene compound does not exchange with benzene-*d*₆ solvent.¹⁸

The exclusive formation of **2-Phenyl** in THF was studied in more detail. Dissolution of brown **2-(N₂)₂** in THF resulted in immediate formation of a purple solution. Collecting the noncombustible gas formed from the dissolution process with a Toepler pump produced 93% of the amount expected for liberation of 2 equiv of dinitrogen. Removal of the solvent yielded a purple solid that was identified on the basis of combustion analysis and NMR spectroscopy as the bis(imino)pyridine iron bis(THF) complex **2-(THF)₂**. Dissolving the isolated purple solid in benzene-*d*₆ under an atmosphere of dinitrogen immediately regenerated **2-(N₂)₂** concomitant with liberation of 2 equiv of THF (eq 9).



The ¹H NMR spectrum of **2-(THF)₂** in THF-*d*₈ or benzene-*d*₆ produced the number of resonances expected for a molecule with idealized C_{2v} symmetry, arising from rapid rocking of the THF ligands through the iron-chelate plane on the time scale of the experiment. Samples prepared in benzene-*d*₆ must be thoroughly degassed of dinitrogen to avoid formation of **2-(N₂)₂**. All of the peaks were assigned on the basis of integration and two-dimensional experiments. As with **2-(N₂)₂**, the protons that lie in the plane of the iron experience the largest shifts. For example, the *meta* pyridine protons appear at 23.83 ppm in THF-*d*₈, and the *para* protons were located at 10.61 ppm. The hydrogens orthogonal to the metal chelate plane appear close to their

Table 6. Relative Rates of Conversion of 2-(THF)₂ to 2-Phenyl in Benzene-*d*₆ at 23 °C as a Function of Added THF

equiv of added THF	time to completion (h) ^a
0	53
2	69
6	108
25	193
neat	36

^a Defined as >98% as judged by ¹H NMR spectroscopy at 23 °C.

Table 7. Formation of 2-Aryl versus 2-Phenyl as a Function of Added Cyclohexene in a 6.1 mM solution of 2-(N₂)₂ in Pentane after Stirring 48 h under Vacuum

[cyclohexene] (mM)	% 2-Aryl	% 2-Phenyl
0	100	0
6.1	75	25
12	63	37
25	47	53

diamagnetic reference values. A complete assignment of the ¹H and ¹³C NMR spectra is reported in the Experimental Section.

Allowing THF-*d*₈ solutions of **2-(THF)₂** to stand at 23 °C resulted in quantitative conversion to **2-Phenyl** after 36 h. To determine the influence of added THF on the rate of **2-Phenyl** formation, the conversion of **2-(THF)₂** to **2-Phenyl** was monitored by ¹H NMR spectroscopy in benzene-*d*₆ as a function of added THF. The relative rates were quantified by measuring the time required to reach >98% conversion because the kinetics are not straightforward (vide infra). As reported in Table 6, adding 2–25 equiv of excess THF inhibits formation of **2-Phenyl**, similar to the behavior observed with dinitrogen for the conversion of **2-(N₂)₂** to **2-Aryl**. However, these data do not fit a simple inverse first-order dependence, and the observation of a *faster* rate of conversion in neat THF-*d*₈ implies a more complex kinetic process perhaps due to competing solvation effects.¹⁹

The observation of exclusive formation of **2-Phenyl** in coordinating solvents prompted investigation of the influence of potential Lewis bases on the selectivity of the arene coordination. As presented in Table 7, increasing the concentration of cyclohexene in a 6.1 mM solution of **2-(N₂)₂** in pentane increased the amount of **2-Phenyl** observed. Because the two iron aryl compounds do not interconvert, the conversion is under kinetic rather than thermodynamic control. Notably, dissolving **2-(N₂)₂** in neat cyclohexene for 5 min, removing the volatiles, and dissolving the residue in benzene-*d*₆ resulted in 88% conversion to **2-Phenyl**. The remaining 12% of the material was identified as residual **2-(N₂)₂**. This observation accounts for the slow rates of hydrogenation to cyclohexane when **2-(N₂)₂** was employed as the catalyst precursor.

In the absence of a detailed study of the electronic structure of **2-(N₂)₂** and observable intermediates, drawing firm mechanistic conclusions from the above data is tenuous. Despite these limitations, it is clear that at least two competitive pathways are operative in the formation of **2-Aryl** and **2-Phenyl**. The data definitively establish that coordinating solvents (THF, cyclohexene) lead exclusively to **2-Phenyl**, suggesting that under these conditions, imine dissociation is operative, allowing competitive C_{ipso}–C_{imine} bond rotation and phenyl coordination. The putative κ^2 -bis(imino)pyridine iron intermediate is most likely stabilized by solvent coordination. Displacement of the solvent molecules from the coordination sphere of the iron could

(19) Attempts were made to monitor the conversion of **2-(N₂)₂** to η^6 -arene compounds in the presence of 1,2-dimethyltetrahydrofuran. However, addition of this solvent produced unidentified iron products.

be rate limiting (or pre-rate limiting) and would account for the observed inhibition by added THF in benzene. However, the observed rate acceleration in neat THF suggests a more complex process. Notably, **2-Phenyl** is the major product in benzene-*d*₆ and toluene, suggesting the intermediacy of η^2 -arene compounds.²⁰ If formed, these intermediates must be displaced by the incoming phenyl substituent of the bis(imino)pyridine ligand, as η^6 -benzene or toluene compounds are not observed. Recall if these complexes were formed, the irreversibility of arene coordination would allow observation and isolation.

Observation of **2-Aryl** and **2-Phenyl** from **2-(N₂)₂** prompted investigation of the stability of the methyl-substituted complex **1-(N₂)₂**. Benzene-*d*₆ and pentane solutions of **1-(N₂)₂** (in equilibrium with **1-N₂**) are stable indefinitely at ambient temperature under 1 atm of dinitrogen. Continued cycles of solvent removal and degassing of a benzene-*d*₆ solution of **1-N₂** resulted in gradual formation of a paramagnetic, red solid. While the paramagnetism of the compound definitively excludes formation of an η^6 -arene complex, the identity of this NMR-silent material remains unknown. Notably, addition of 1 atm of dinitrogen regenerates **1-(N₂)₂**, suggesting that the NMR-silent compound is the bis(imino)pyridine iron cyclometalated hydride implicated in deuterium-labeling studies.⁸ Experiments are ongoing to definitively establish the identity of this compound.

In summary, the data reported in this study demonstrate how subtle manipulation of the backbone architecture of bis(imino)pyridine ligands induces arene coordination to form catalytically inactive η^6 -arene complexes. For the phenyl-substituted dinitrogen complex **2-(N₂)₂**, coordination of the imine aryl and backbone phenyl is solvent dependent. The latter was observed in the presence of coordinating solvents such as THF, suggesting stabilization of a κ^2 -bis(imino)pyridine intermediate allowing C_{ipso}–C_{imine} bond rotation.

Experimental Section

General Considerations. All air- and moisture-sensitive manipulations were carried out using standard vacuum line, Schlenk, and cannula techniques or in an MBraun inert atmosphere drybox containing an atmosphere of purified nitrogen. The MBraun drybox was equipped with a cold well designed for freezing samples in liquid nitrogen. Solvents for air- and moisture-sensitive manipulations were initially dried and deoxygenated using literature procedures.²¹ Argon and hydrogen gas were purchased from Airgas Incorporated and passed through a column containing manganese oxide supported on vermiculite and 4 Å molecular sieves before admission to the high-vacuum line. Benzene-*d*₆ was purchased from Cambridge Isotope Laboratories and distilled from sodium metal under an atmosphere of argon and stored over 4 Å molecular sieves or sodium metal.

¹H NMR spectra were recorded on Varian Mercury 300 and Inova 400 and 500 spectrometers operating at 299.763, 399.780, and 500.62 MHz, respectively. All chemical shifts are reported relative to SiMe₄ using ¹H (residual) chemical shifts of the solvent as a secondary standard. For paramagnetic molecules, the ¹H NMR data are reported with the chemical shift followed by the peak width at half-height in hertz or multiplicity, followed by integration value and, where possible, peak assignment. Magnetic moments as determined by the Evans method²² using a ferrocene standard and are the mean value of at least two independent measurements, unless stated otherwise.

Single crystals suitable for X-ray diffraction were coated with polyisobutylene oil in a drybox and were quickly transferred to

the goniometer head of a Bruker X8 APEX2 system equipped with a molybdenum X-ray tube ($\lambda = 0.71073$ Å). Preliminary data revealed the crystal system. A hemisphere routine was used for data collection and determination of lattice constants. The space group was identified and the data were processed using the Bruker SAINT program and corrected for absorption using SADABS. The structures were solved using direct methods (SHELXS), completed by subsequent Fourier synthesis, and refined by full-matrix least-squares procedures. Elemental analyses were performed at Robertson Microлит Laboratories, Inc., in Madison, NJ. The general procedures for catalytic olefin hydrogenation and hydrosilylation were carried out as described previously in pentane rather than toluene solution.⁸

All calculations were performed with the Amsterdam Density Functional Theory (ADF2003.01) suite of programs.^{23–25} Relativistic effects were included using the zero-order regular approximation. The Vosko, Wilk, and Nusair (VWN) local density approximation,²⁶ Becke's exchange,²⁷ and Perdew's correlation²⁸ (BP86) were used. The cores of the atoms were frozen up to 1s for C and N and 2p for Fe. Uncontracted Slater-type orbitals (STOs) of triple- ζ quality with two polarizations were employed. This basis set is denoted TZ2P in the ADF program. Each geometry optimization was carried out without symmetry constraints. Orbital representations were generated using ADF view.

Preparation of (ⁱPrPhPDI)FeCl₂ (2-Cl₂). A 500 mL round-bottomed flask was charged with 3.560 g (11.67 mmol) of 2,6-dibenzoylpyridine. A solution of 4.149 g (23.40 mmol) of 2,6-diisopropylaniline dissolved in 150 mL of acetic acid and the resulting yellow solution was heated to reflux. Under a stream of argon gas, 1.483 g (11.70 mmol) of FeCl₂ was added to the stirring mixture, forming a blue slurry. Following the addition, the reflux was resumed for 4 h, after which time the mixture was cooled to room temperature. Acetic acid from the blue mixture was removed in vacuo on a Schlenk line. Residual solvent was removed under high vacuum. In the dry box, the resulting blue solid was dissolved in a minimal amount of anhydrous dichloromethane, precipitated by layering with pentane, and recovered on a filter. The filter cake was washed with three 20 mL portions of diethyl ether and three 20 mL portions of pentane and then dried under vacuum, yielding 5.959 g (70%) of a dark blue powder identified as **2-Cl₂**. Anal. Calcd for C₄₃H₄₇N₃FeCl₂: C, 70.50; H, 6.47; N, 5.74. Found: C, 70.39; H, 6.75; N, 5.75. Magnetic susceptibility: $\mu_{\text{eff}} = 5.9$ μB (solid-state balance). ¹H NMR (dichloromethane-*d*₂, 22 °C): δ –18.63 (519, 4H, CHMe₂), –9.22 (24, 2H, *p*-Ar), –6.12 (40, 12H, CHMe₂), 1.41 (d, 88 Hz, 12H, CHMe₂), 7.07 (190, 2H, *p*-Ph), 7.40 (36, 4H, 36, *m/o*-Ph), 8.08 (21, 4H, *m/o*-Ph), 14.42 (46, 4H, *m*-Ar), 77.97 (60, 2H, *m*-Pyr), 82.36 (40, 1H, *p*-Pyr).

Preparation of (ⁱPrPhPDI)FeBr₂ (2-Br₂). This compound was prepared using the method described for **2-Cl₂** with 1.270 g (4.49 mmol) of 2,6-dibenzoylpyridine, 1.770 g (9.97 mmol) of 2,6-

(22) Sur, S. K. *J. Magn. Reson.* **1989**, *82*, 169.

(23) Velde, G. T.; Bickelhaupt, F. M.; Baerends, E. J.; Guerra, C. F.; van Gisbergen, S. J. A.; Snijders, J. G.; Ziegler, T. *J. Comput. Chem.* **2001**, *22*, 931.

(24) Fonseca Guerra, C.; Snijders, J. G.; te Velde, G.; Baerend E. J. *Theor. Chem. Acc.* **1998**, *99*, 391.

(25) Baerends, E. J.; Autschbach, J. A.; Berces, A.; Bo, C.; Boerrigter, P. M.; Cavallo, L.; Chong, D. P.; Deng, L.; Dickson, R. M.; Ellis, D. E.; Fan, L.; Fischer, T. H.; Guerra Fonseca, C.; van Gisbergen, S. J. A.; Groeneveld, J. A.; Gritsenko, O. V.; Grüning, M.; Harris, F. E.; van den Hoek, P.; Jacobsen, H.; van Kessel, G.; Koostra, F.; van Lenthe, E.; Osinga, V. P.; Patchkovshii, S.; Philipsen, P. H. T.; Post, D.; Pye, C. C.; Ravenek, W.; Ros, P.; Schipper, P. R. T.; Schreckenbach, G.; Snijders, J. G.; Sola, M.; Swart, M.; Swerhone, D.; te Velde, G.; Vernooijs, P.; Versluis, L.; Visser, O.; van Wezenbeek, E.; Wiesenekker, G.; Wolff, S. K.; Woo, T. K.; Ziegler, T. *ADF 2002.03*; SCM Theoretical Chemistry, Vrije Universiteit: Amsterdam, The Netherlands, <http://www.scm.com/>.

(26) Vosko, S. H.; Wilk, L.; Nusair, M. *Can. J. Phys.* **1990**, *58*, 1200.

(27) Becke, A. D. *Phys. Rev.* **1988**, *A38*, 2398.

(28) Perdew, J. P. *Phys. Rev.* **1986**, *B33*, 8822.

(20) For an example of η^2 -coordination in iron chemistry see: Sciarone, T. J. J.; Meetsma, A.; Hessen, B.; Teuben, J. H. *Chem. Commun.* **2002**, 1580.

(21) Pangborn, A. B.; Giardello, M. A.; Grubbs, R. H.; Rosen, R. K.; Timmers, F. J. *Organometallics* **1996**, *15*, 1518.

diisopropylaniline, and 0.970 g (4.49 mmol) of FeBr_2 , yielding 2.093 g (57%) of a dark blue powder identified as **2-Br₂**. Anal. Calcd for $\text{C}_{43}\text{H}_{47}\text{N}_3\text{FeBr}_2$: C, 62.87; H, 5.77; N, 5.12. Found: C, 62.69; H, 5.54; N, 5.00. Magnetic susceptibility: $\mu_{\text{eff}} = 5.4 \mu\text{B}$ (solid-state balance). ^1H NMR (benzene- d_6 , 22 °C): δ -16.38 (445, 4H, CHMe_2), -9.86 (26, 2H, *p*-Ar), -5.86 (55, 12H, CHMe_2), -5.44 (303, 12H, CHMe_2), 6.87 (36, 4H, *m/o*-Ph), 8.89 (22, 2H, *p*-Ph), 9.20 (237, 4H, *m/o*-Ph), 14.35 (40, 4H, *m*-Ar), 74.64 (74, 2H, *m*-Pyr), 101.56 (60, 1H, *p*-Pyr).

Preparation of ($^{\text{Pr}}$ PhPDI)Fe(N_2)₂ (2-(N₂)₂**).** A thick walled glass vessel was charged with 44.62 g of mercury, approximately 100 mL of pentane, and a magnetic stir bar. Sodium metal (0.224 g, 9.76 mmol, 0.5 wt %) was added to the vessel in small (~20 mg) portions. The resulting slurry was stirred for 15 min to completely dissolve the metal. After this time, a pentane slurry containing 1.429 g (1.024 mmol) of **2-Cl₂** was added to the vessel. The vessel was sealed, cooled to liquid nitrogen temperature, and evacuated on a Schlenk line. At -196 °C, 1 atm of N_2 was added. The vessel was resealed and warmed to ambient temperature. The resulting reaction mixture was stirred for 24 h, after which time a brown solution was decanted from the amalgam. The remaining product was extracted from the amalgam into pentane and filtered through Celite, and the solvent from the combined organic layers was removed in vacuo. The resulting brown solid was recrystallized from pentane at -35 °C, yielding 0.558 g (40%) of **2-(N₂)₂**. Anal. Calcd for $\text{C}_{43}\text{H}_{47}\text{N}_7\text{Fe}$: C, 71.96; H, 6.60; N, 13.66. Found: C, 71.98; H, 6.64; N, 13.36. IR (KBr) ν_{N_2} : 2074, 2130 cm^{-1} . IR (pentane, -78 °C) ν_{N_2} : 2086, 2138 cm^{-1} . Characterization of **2-N₂**: IR (pentane, 23 °C) $\nu_{\text{N}_2} = 2061 \text{ cm}^{-1}$. ^1H NMR (benzene- d_6 , 23 °C): δ -0.80 (t, 8 Hz, 1H, *p*-Pyr), -0.71 (d, 6 Hz, 12H, CHMe_2), 0.05 (sept, 6 Hz, 4H, CHMe_2), 1.16 (d, 6 Hz, 12H, CHMe_2), 4.61 (t, 8 Hz, 2H, *p*-Ph), 5.82 (d, 8 Hz, 4H, *o*-Ph), 7.80 (t, 8 Hz, 2H, *p*-Ar), 8.05 (d, 8 Hz, 4H, *m*-Ar), 8.13 (t, 8 Hz, 4H, *m*-Ph), 11.80 (d, 8 Hz, 2H, *m*-Pyr). ^{13}C NMR (benzene- d_6 , 22 °C): δ 24.79 (CHMe_2), 40.27 (CHMe_2), 52.18 (CHMe_2), 122.85, 124.80, 125.25, 128.06, 130.51, 144.15, 173.57.

Preparation of ($^{\text{Pr}}$ PhPDI)Fe(CO)₂ (2-(CO)₂**).** A thick walled glass vessel was charged with 6.245 g of mercury, approximately 10 mL of pentane, and a stir bar. Sodium metal (0.031 g, 1.4 mmol) was added to the vessel in small (~15 mg) portions. The resulting slurry was stirred for 10 min to ensure complete dissolution of the metal. A pentane slurry containing 0.200 g (0.273 mmol) of **2-Cl₂** was added to the flask containing the amalgam. The vessel was sealed, cooled to liquid nitrogen temperature, and evacuated. At this temperature 1 atm of CO was added. The reaction mixture was stirred vigorously for 24 h. The yellowish-brown solution in the resulting mixture was decanted away from the amalgam. Pentane was used to extract the remaining product from the amalgam, and both portions were combined and filtered through Celite to remove NaCl. The filtrate was collected and the solvent was removed in vacuo, yielding 0.121 g (62%) a yellowish-brown solid identified as **2-(CO)₂**. Anal. Calcd for $\text{C}_{45}\text{H}_{47}\text{N}_3\text{O}_2\text{Fe}$: C, 75.31; H, 6.60; N, 5.85. Found: C, 74.97; H, 7.00; N, 5.98. IR (KBr, 23 °C) ν_{CO} : 1979, 1921 cm^{-1} . IR (pentane, 23 °C) ν_{CO} : 1979, 1921 cm^{-1} . ^1H NMR (benzene- d_6 , 22 °C): δ 0.92 (d, 7 Hz, 12H, CHMe_2), 1.25 (t, 8 Hz, 1H, *p*-Pyr), 1.55 (d, 7 Hz, 12H, CHMe_2), 3.18 (spt, 7 Hz, 4H, CHMe_2), 7.02-7.27 (16H, Ph and Ar), 7.62 (d, 8 Hz, 2H, *m*-Pyr). ^{13}C NMR (benzene- d_6 , 22 °C): δ 24.45 (CHMe_2), 26.84 (CHMe_2), 28.93 (CHMe_2), 121.49, 124.39, 125.69, 127.50, 128.45, 128.90, 131.78, 135.24, 141.11, 148.10, 151.05, 158.68.

Preparation of 2-Aryl. A 50 mL round-bottomed flask was charged with 6.245 g of Hg and approximately 500 mL of pentane. Sodium metal (0.031 g, 1.37 mmol) was added to the flask. The resulting amalgam was stirred for 10 min. After this time, a pentane slurry containing 0.200 g (0.273 mmol) of **2-Cl₂** was added to the amalgam. The resulting blue reaction mixture was stirred vigorously for 72 h and the solution decanted away from the amalgam. The

remaining product was extracted from the amalgam with pentane, and the extracts were combined and filtered through Celite to remove NaCl. The filtrate was collected and the solvent removed in vacuo to yield 0.130 g (72%) of a red solid identified as **2-Aryl**. Anal. Calcd for $\text{C}_{43}\text{H}_{47}\text{N}_3\text{Fe}$: C, 78.05; H, 7.16; N, 6.35. Found: C, 77.95; H, 7.43; N, 6.59. ^1H NMR (benzene- d_6): δ 0.71 (d, 7 Hz, 6H, CHMe_2^*), 1.17 (d, 7 Hz, 6H, CHMe_2), 1.27 (d, 7 Hz, 6H, CHMe_2), 1.49 (d, 7 Hz, 6H, CHMe_2^*), 3.45 (spt, 7 Hz, 2H, CHMe_2), 3.65 (spt, 7 Hz, 2H, CHMe_2^*), 4.36 (t, 6 Hz, 1H, *p*-Ar*), 5.63 (d, 6 Hz, 2H, *m*-Ar*), 6.32 (dd, 8 and 7 Hz, 1H, *p*-Pyr), 6.74-6.83 (m, 5H, Ph*), 6.92 (dd, 8 Hz & 1 Hz, 1H, *m*-Pyr*), 7.03 (d, 7 Hz, 2H, *o*-Ph), 7.25 (t, 7 Hz, 2H, *m*-Ph), 7.32 (dd, 7 and 1 Hz, 1H, *m*-Pyr), 7.35 (m, 2H, *p*-Ar and *p*-Ph), 7.94 (d, 8 Hz, 2H, *m*-Ar). ^{13}C NMR (benzene- d_6 , 22 °C): δ 22.39 (CHMe_2), 23.15 (CHMe_2), 24.10 (CHMe_2^*), 25.84 (CHMe_2^*), 27.90 (CHMe_2^*), 28.30 (CHMe_2), 79.49 (*p*-Ar*), 80.34 (*m*-Ar*), 83.48 (*o*-Ar*), 109.38 (ipso-Ar*), 118.59 (*p*-Pyr), 123.52 (Ph), 126.02 (Ph), 126.11 (Ph), 127.49 (Ph), 128.97 (*m*-Pyr), 129.46 (*m*-Ar), 130.42 (Ph), 132.42 (Ph), 135.81, 141.43, 143.88, 144.09, 148.19, 149.37, 153.16, 175.31. * denotes resonances on the portion of the molecule where the arene is coordinated to iron.

Preparation of 2-Phenyl. A J. Young NMR tube was charged with 0.017 g (0.024 mmol) of **2-(N₂)₂** and approximately 0.5 mL of dry tetrahydrofuran. The tube was immersed in a liquid nitrogen bath and evacuated on the high-vacuum line. The contents were then warmed to ambient temperature and shaken for 48 h. Solvent was removed in vacuo, yielding a red oil. A minimal quantity of pentane was used to extract the oil from the tube and was placed in a 20 mL scintillation vial. The pentane was removed in vacuo, affording 0.015 g (94%) of an orange oil identified as **2-Phenyl**. Crystals suitable for X-ray analysis were grown from a pentane solution at -35 °C. Anal. Calcd for $\text{C}_{43}\text{H}_{47}\text{N}_3\text{Fe}$: C, 78.05; H, 7.16; N, 6.35. Found: C, 77.72; H, 6.85; N, 5.95. ^1H NMR (benzene- d_6 , 22 °C): δ 0.80 (d, 7 Hz, 6H, CHMe_2), 1.27 (d, 6H, 7 Hz, CHMe_2), 1.37 (d, 12H, 7 Hz, CHMe_2), 3.26 (spt, 2H, 7 Hz, CHMe_2), 3.55 (spt, 7 Hz, 2H, CHMe_2), 3.85 (t, 6 Hz, 1H, *p*-Ph*), 5.32 (t, 6 Hz, 2H, *m*-Ph*), 5.66 (d, 6 Hz, 2H, *o*-Ph*), 6.47 (dd, 8 and 7 Hz, 1H, *p*-Pyr), 6.83 (d, 7 Hz, 2H, *o*-Ph), 6.87 (t, 7 Hz, 1H, *p*-Ph), 6.93 (t, 7 Hz, 2H, *m*-Ph), 7.05 (t, 7 Hz, 1H, *p*-Ar), 7.11 (d, 7 Hz, 2H, *m*-Ar), 7.14 (d, 9 Hz, 2H, *m*-Ar), 7.16-7.25 (m, 2H, *p*-Ar and *m*-Pyr), 7.58 (dd, 7 and 1 Hz, 1H, *m*-Pyr). ^{13}C NMR (benzene- d_6 , 22 °C): δ 22.90 (CHMe_2), 24.61 (CHMe_2), 24.88 (CHMe_2), 26.59 (CHMe_2), 28.52 (CHMe_2), 29.66 (CHMe_2), 80.27 (*p*-Ph*), 83.96 (*o*-Ph*), 85.91 (*m*-Ph*), 89.71 (ipso-Ph*), 109.81, 122.89, 123.96, 124.07, 125.45, 126.41, 126.47, 129.03, 129.51, 135.87, 136.50, 142.33, 144.54, 147.47, 149.60, 153.35, 166.72, 167.95. * denotes resonances on the portion of the molecule where the phenyl group is coordinated to iron.

Preparation of ($^{\text{Pr}}$ PhPDI)Fe(THF)₂ (2-(THF)₂**).** A 20 mL scintillation vial was charged with 0.017 g (0.024 mmol) of **2-(N₂)₂** and approximately 2 mL of THF. The resulting purple solution was stirred for 5 min. The volatiles were removed in vacuo, yielding 0.019 g (97%) of purple solid identified as **2-(THF)₂**. Anal. Calcd for $\text{C}_{51}\text{H}_{61}\text{N}_3\text{O}_2\text{Fe}$: C, 76.20; H, 7.65; N, 5.23. Found: C, 75.87; H, 7.75; N, 4.83. ^1H NMR (THF- d_8 , 22 °C): δ -2.42 (30, 4H, CHMe_2), -0.99 (13, 12H, CHMe_2), 0.39 (20, 12H, CHMe_2), 6.67 (26, 4H, *m*-Ph), 6.84 (26, 2H, *p*-Ph), 7.68 (19, 4H, *o*-Ph), 9.51 (25, 2H, *p*-Ar), 10.29 (23, 4H, *m*-Ar), 10.61 (25, 1H, *p*-Pyr), 22.83 (24, 2H, *m*-Pyr). ^2H NMR (THF- d_8 , 22 °C): δ 1.14 (66, 4D, 2,3-THF), 3.00 (5, 4D, 1,4-THF). ^{13}C NMR (THF- d_8 , 22 °C): δ 14.45 (CHMe_2), 23.28 (CHMe_2), 24.06 (broad, 13 Hz, 2,3-THF), 30.00 (broad, 19 Hz, 1,4-THF), 35.13 (CHMe_2), 93.98, 116.17, 119.89, 132.83, 134.51, 140.97. ^1H NMR (benzene- d_6 , 23 °C): δ -2.26 (25, 4H, CHMe_2), -0.84 (11, 12H, CHMe_2), 0.51 (10, 12H, CHMe_2), 1.44 (69, 8H, 2,3-THF), 3.59 (63, 8H, 1,4-THF), 6.67 (t, 7.7 Hz, 4H, *m*-Ph), 6.96 (t, 7.7 Hz, 2H, *p*-Ph), 7.63 (d, 7.6 Hz, 4H,

o-Ph), 9.13 (t, 7.6 Hz, 2H, *p*-Ar), 10.12 (d, 7.6 Hz, 4H, *m*-Ar), 10.44 (t, 7.6 Hz, 1H, *p*-Pyr), 21.35 (17, 2H, *m*-Pyr).

Preparation of (¹²⁹PrMeOPDI)FeBr₂ (3-Br₂). A 100 mL round-bottomed flask was charged with 0.30 g (1.4 mmol) of FeBr₂ and 0.72 g (1.4 mmol) of ¹²⁹PrMeOPDI and fitted with a 180° needle valve. On the vacuum line, approximately 50 mL of THF was condensed onto the solids at -78 °C, and the resulting mixture was warmed to ambient temperature and stirred for 2 days. During this time, a pink reaction mixture formed. The solvent was removed in vacuo and the resulting pink residue was washed with pentane to afford 0.89 g (88%) of a pink solid identified as **3-Br₂**. ¹H NMR (dichloromethane-*d*₂): δ -30.9 (1765.0), -18.9 (1451.2), 0 to -15 (at least 3 broad overlapping), 12.5 (927.7), 24.6 (851.0), 29.1 (1005.8), 56.7 (793.8), 82.0-87.5 (3 broad overlapping), 90.1 (932.2). Magnetic susceptibility: μ_{eff} = 5.1 μB (solid-state balance). MS (*m/z*) calcd = 727.10717, found = 727.10570.

Preparation of 3-Aryl. A 20 mL scintillation vial was charged with 6.40 g (32.0 mmol) of mercury and approximately 15 mL of pentane. To this suspension was added 0.036 g (1.57 mmol) of sodium. The resulting amalgam was stirred for 10 min. A pentane slurry containing 0.200 g (0.28 mmol) of **3-Br₂** was added to the flask containing the amalgam. The resulting reaction mixture was stirred vigorously, forming a red-brown solution. After 18 h, the solution was decanted from the amalgam and the maroon liquid was filtered through Celite. The solvent was removed in vacuo and the resulting residue recrystallized from a pentane/toluene (~2:1) mixture, yielding 0.060 g (39%) of a maroon solid identified as **3-Aryl**. Anal. Calcd for C₃₃H₄₃N₃O₂Fe: C, 69.94; H, 7.64; N, 7.42. Found: C, 69.17; H, 7.29; N, 7.01. ¹H NMR (benzene-*d*₆, 22 °C) δ 1.16 (d, 7.2 Hz, 3H, CHMe₂), 1.20 (d, 7.2 Hz, 3H, CHMe₂), 1.26 (d, 7.2 Hz, 3H, CHMe₂), 1.52 (d, 7.2 Hz, 3H, CHMe₂), 2.96 (s, 3H, OCH₃), 3.31 (spt, 7.2 Hz, 2H, CHMe₂), 3.43 (spt, 7.2 Hz, 2H, CHMe₂), 4.02 (s, 3H, OCH₃), 4.11 (t, 6.4 Hz, 1H, *p*-aryl), 5.53 (d, 6.4 Hz, 2H, *m*-aryl), 6.53 (t, 8.4 Hz, 1H, *p*-Pyr), 6.66 (d, 8.4 Hz, 2H, *m*-Pyr), 7.26-7.38 (*m*-aryl, *p*-aryl), 7.94 (d, 7.2 Hz, 1H, *m*-Pyr). ¹³C NMR (benzene-*d*₆, 22 °C): δ 22.32 (CHMe₂), 23.50 (CHMe₂), 25.17 (CHMe₂), 25.64 (CHMe₂), 28.00 (CHMe₂), 28.18 (CHMe₂), 54.31 (OCH₃), 59.56 (OCH₃), 78.33 (*m*-Ar), 78.75 (*p*-Ar), 116.04 (*p*-Pyr), 122.056 (*m*-Pyr), 123.36 (*m*-Ar), 126.05 (*p*-Ar), 129.74 (*m*-Pyr).

Preparation of (¹²⁹PrMeOPDI)Fe(CO)₂ (3-(CO)₂). A J. Young NMR tube was charged with a solution of **3-Aryl** in benzene-*d*₆ and attached to a high-vacuum line. The solution was degassed, and 4 atm of CO was added. The solution was shaken overnight, affording a green solution of a compound identified as **3-(CO)₂**. ¹H NMR (benzene-*d*₆): δ 1.18 (d, 7 Hz, 12H, CH₂Me), 1.50 (d, 7 Hz, 12H, CH₂Me), 2.93 (sept, 7 Hz, 4H, CHMe₂), 3.39 (s, 6H, OMe), 6.89 (t, 8 Hz, *p*-pyr), 7.0-7.2 (*p*-aryl and *m*-aryl), 7.69 (d, 8 Hz, 2H, *m*-pyr). IR (pentane): ν_{CO} = 2013, 1974, 1957, 1933, 1912 cm⁻¹.

Preparation of 2,6-(2,6-¹²⁹Pr₂C₆H₃N=C(OEt))₂C₅H₃N. A 250 mL round-bottomed flask was charged with 2.50 g (0.037 mol) of NaOEt and 3.57 g (6.80 mmol) of *N,N'*-bis(2,6-diisopropylphenyl)pyridine-2,6-carboximidoyl chloride. A reflux condenser and 180° needle valve were attached. On the Schlenk line, the contents of the assembly were degassed, and approximately 100 mL of THF was added to the solids by vacuum transfer. The resulting solution was heated to reflux temperature for 3 days. After this time, the volatiles were removed in vacuo and the resulting yellow residue was dissolved in approximately 50 mL of CH₂Cl₂ and washed with approximately 40 mL of 2 M NaOH, 40 mL of H₂O, and 40 mL of brine. The organic layer was dried over Na₂SO₄ and the solvent removed by Rotovap, yielding 2.88 g (78%) of a burnt-orange solid identified as ¹²⁹PrEtOPDI. MS (*m/z*) calcd = 541.3668, found = 541.3670. ¹H NMR (chloroform-*d*, 22 °C): δ 0.94 (d, 7.1 Hz, 12H,

CHMe₂), 1.14 (d, 7.1 Hz, 12H, CHMe₂), 1.34 (br, 4H, OCH₂CH₃), 2.90 (spt, 7.1 Hz, 4H, CHMe₂), 4.32 (br, 4H, OCH₂CH₃), 7.0-7.1 (*m*-Ar, *p*-Ar), 7.2-7.6 (br, *m*-Pyr, *p*-Pyr). ¹³C NMR (chloroform-*d*, 22 °C): δ 14.5 (OCH₂CH₃), 22.4 (CHMe₂), 23.4 (CHMe₂), 28.1 (CHMe₂), 62.7 (OCH₂CH₃), 122.6 (*m*-aryl), 124.4 (*p*-aryl), 136.2 (*p*-Pyr), 137.0 (*m*-Pyr), 142.7 (*o*-Ar), 149.8 (*ipso*-Ar), 153.8 (*o*-Pyr).

Preparation of (¹²⁹PrEtOPDI)FeBr₂ (4-Br₂). This compound was prepared in a manner identical to **3-Br₂** with 1.10 g (5.10 mmol) of FeBr₂ and 2.79 g (5.13 mmol) of ¹²⁹PrEtOPDI and yielded 3.70 g (95%) of a blue solid identified as **4-Br₂**. ¹H NMR (dichloromethane-*d*₂): δ -32.8 (309.1, 4H), -16.4 (832.2, 4H), -10.7 (349.7, 12H, CHMe₂), -8.6 to -5.0 (2 broad overlapping, 14H), -3.5 (489.8, 6H, OCH₂CH₃), 13.3 (300.9, 4H), 31.2 (198.7, 1H, *p*-Pyr), 83.7 (253.6, 2H). Magnetic susceptibility (solid-state balance, 23 °C): μ_{eff} = 5.2 μB. MS (*m/z*) calcd = 755.13847, found = 755.13811.

Preparation of 4-Aryl. A 100 mL round-bottomed flask was charged with 14.15 g (70.7 mmol) of Hg and approximately 50 mL of pentane. To the slurry was added 0.075 g (3.3 mmol) of sodium metal. The resulting amalgam was stirred for 10 min to completely dissolve the metal. A pentane slurry containing 0.451 g (0.59 mmol) of **4-Br₂** was added and the resulting reaction mixture stirred vigorously, forming a red-brown mixture. After 26 h, the solution was decanted from the amalgam and filtered through Celite. The Celite was extracted with pentane and the solvent from the combined extracts removed to yield a maroon solid. Recrystallization from a pentane/toluene (2:1) mixture yielded 0.190 g (53%) of a forest green solid identified as **4-Aryl**. Anal. Calcd for C₃₅H₄₇N₃O₂Fe: C, 70.04; H, 7.90; N, 7.00. Found: C, 69.83; H, 7.81; N, 8.77. ¹H NMR (benzene-*d*₆, 22 °C): δ 0.63 (t, 7.1 Hz, 3H, OCH₂CH₃), 1.18 (d, 7.1 Hz, 3H, CHMe₂), 1.22 (d, 7.1 Hz, 3H, CHMe₂), 1.29 (d, 7.1 Hz, 3H, CHMe₂), 1.41 (t, 7.1 Hz, 3H, OCH₂CH₃), 1.53 (d, 7.1 Hz, 3H, CHMe₂), 3.28 (q, 7.1 Hz, 2H, OCH₂CH₃), 3.38 (spt, 6.7 Hz, 2H, CHMe₂), 3.49 (spt, 6.7 Hz, 2H, CHMe₂), 4.19 (t, 6.7 Hz, 1H, *p*-Ar), 4.64 (q, 7.1 Hz, 2H, OCH₂CH₃), 5.57 (d, 6.65 Hz, 2H, *m*-Ar), 6.58 (ps t, 7.2 8.2 Hz, 1H, *p*-Pyr), 6.77 (dd, 8.2 1.8 Hz, 1H, *m*-Pyr), 7.27-7.38 (3H, *m*-Ar, *p*-Ar), 8.02 (dd, 7.2 1.8 Hz, 1H, *m*-Pyr). ¹³C NMR (benzene-*d*₆, 22 °C): δ 22.52 (CHMe₂), 23.56 (CHMe₂), 24.88 (CHMe₂), 26.05 (CHMe₂), 27.96 (CHMe₂), 28.24 (CHMe₂), 62.82 (OCH₂CH₃), 67.59 (OCH₂CH₃), 78.28 (*p*-aryl), 78.46 (*m*-aryl), 116.22 (*p*-Pyr), 122.26 (*m*-Pyr), 123.41 (*m*-Ar), 126.00 (*p*-Ar), 129.80 (*m*-Pyr).

Preparation of (¹²⁹PrEtOPDI)Fe(CO)₂ (4-(CO)₂). On a high-vacuum line, 4 atm of CO were added to an NMR tube charged with a benzene-*d*₆ solution of **4-Aryl**. The resulting reaction mixture was shaken overnight, affording a dark green solution of a compound identified as **4-(CO)₂**. ¹H NMR (benzene-*d*₆, 22 °C): δ 0.78 (t, 7.1 Hz, 3H, OCH₂CH₃), 1.16 (d, 7.0 Hz, 12H, CHMe₂), 1.47 (d, 7.0 Hz, 12H, CHMe₂), 2.91 (sept, 7.0 Hz, 4H, CHMe₂), 3.72 (q, 7.1 Hz, 4H, OCH₂CH₃), 6.94 (t, 7.7 Hz, 2H, *p*-Ar), 7.0-7.2 (*m*-Ar, *p*-Pyr), 7.75 (d, 7.8, 2H, *m*-Pyr). IR (pentane) ν_{CO}: 2013 (s), 1974 (s), 1957 (m), 1933 (m), 1912 (s) cm⁻¹.

Acknowledgment. We thank the David and Lucile Packard Foundation for financial support. P.J.C. is a Cottrell Scholar of the Research Corporation and a Camille Dreyfus Teacher-Scholar. We also thank Mr. Jim McNeil (Ithaca College) for access to a magnetic susceptibility balance.

Supporting Information Available: Structural data for **2-(N₂)₂**, **2-Aryl**, and **2-Phenyl** as CIF files. This material is available free of charge via the Internet at <http://pubs.acs.org>.

OM060441C